Predicting the Tensile Properties of UV Degraded Nylon66/Polyester Woven Fabric Using Regression and Artificial Neural Network Models

Meysam Moezzi, Mohammad Ghane, Dariush Semnani

Isfahan University of Technology, Department of Textile Engineering, Isfahan, Isfahan IRAN

Correspondence to:
Mohammad Ghane email:m-ghane@cc.iut.ac.ir

ABSTRACT

UV radiation is the major source of radiation in environmental conditions and affects many characteristics of exposed fabrics. Physical properties of polymeric material and fabric deteriorate when exposed to environmental conditions. The study of the changes in physical properties has been a major issue for researchers. Color absorption of degraded fabrics varies with exposure time. The main aim of this work was to predict the physical properties of UV degraded woven fabrics at different levels of exposure time. Samples of plain-woven fabrics were selected. The fabric consisted of nylon 66 as weft yarns and polyester as warp yarns. A UV light source was used to induce controlled degradation at different exposure times. The samples were dyed in identical conditions and the color values for all samples were measured using a spectrophotometer. The samples were then tested with tensile testing machine and stress-strain curves were obtained. Six parameters were considered in stress-strain curves. Exposure time caused the differences in the color values of the samples. This was used to evaluate the tensile behavior. Regression and artificial neural network methods were used to correlate each of the six parameters of tensile properties with color values. To validate the methods, experimental samples were tested with the tensile testing machine and the results were compared with the predicted values. The results show a good agreement between the experimental and predicted models.

Keywords: UV degradation, color values, fabric tensile behavior, regression analysis, artificial neural network

INTRODUCTION

In the study of fabric behavior, it is usually assumed that the fabric is homogenous. However, in practice, there are some sources of local irregularities in fabric such as mass irregularity of the yarns [1]. In general, irregularity in textiles is classified in two categories; a) irregularity in the production process and b) irregularity as a result of exposure to environmental conditions**.** Textile materials are usually designed and produced to be used in outer environmental conditions where the fabrics are subjected to different sources of radiation. One of the most important sources of radiation in the environmental condition is UV radiation. It can affect many properties of the materials including the tensile behavior [2]. Many researchers have studied the effect of UV radiation on the mechanical properties of textile fabrics. Zhang et al studied the effects of solar UV irradiation on the tensile properties and the structure of PPTA fibers [3]. Exposure of UV radiation was found to affect the internal structure the fibers. Change in internal structure of the fibers leads to variation of color absorption behavior [4-6]. Thus, color values can be used as a criterion to evaluate the mechanical properties of the materials.

The Tensile stress-strain behavior of textiles has been studied widely [7-9]. Serwatka et al presented a new approach for modeling the stress-strain curve of the yarns [10]. Regression is the one of the most famous methods in assessing the experimental data. It has been used in predicting the fabric physical property in several years [11]. Abghari et al suggested a 3D regression method to predict woven fabric bagging behavior from in-plane fabric tensile properties [12]. Almetwally et al proposed a regression method to Compare Mechanical Properties of fabrics woven from compact and ring spun yarns [13]. Malik et al developed models to predict the tensile strength of cotton woven fabrics [14]. Kotb presented a deepened understanding of plain-woven fabrics using regression analysis [15]. Kannappan et al used the quadratic regression model to correlate the Process Variables to the Tensile Properties of Short Jute Fiber Reinforced with Polypropylene Composite Board [16].

The nature of such a complex system prevents predicting the final properties of the fabrics. Some modeling methods, such as phenomenological, empirical, statistical regression, semi empirical, and numerical models give reasonable responses from an industrial point of view, but there is a mathematical modeling called artificial neural network (ANN) which has been used widely for nonlinear processes recently. Zeydan et al modeled the woven fabrics strength using artificial neural network and Taguchi methodologies [17]. Ertugrul and Ucar predicted the strength of plain knitted fabric with fabric weight, strength and elongation of fabric by using feed forward neural network and ANFIS algorithms [18]. Hadizadeh et al predicted the initial load-extension behavior of woven fabrics using artificial neural network and adaptive neuro- fuzzy system [19, 20].

The aim of this study was to use multiple regression and ANN methods for predicting the tensile properties of UV degraded fabrics. Color values of the fabrics were used as independent variables to predict the tensile parameters. Regression and artificial neural network methods were used to correlate each of the six tensile property parameters with color values. In order to validate the models, the predicted values were then compared with the experimental results.

THEORY

Neural Network Model and Back Propagation Algorithm

The multi-layered ANN model is an information process that can be used for simulating the treatment of nonlinear and complex systems [21]. The structure of multi layered ANN can consist of different layers of input, middle or hidden, and output layers. The input layer receives and distributes the input signals. In the hidden layers, the relation between the input and output layers is created, and the output layer gives the output value. The number of neurons in the input and output layers depends on the number of problem parameters, and there is no order to exactly determine it. *Figure 1* shows the ANN with one hidden layer.

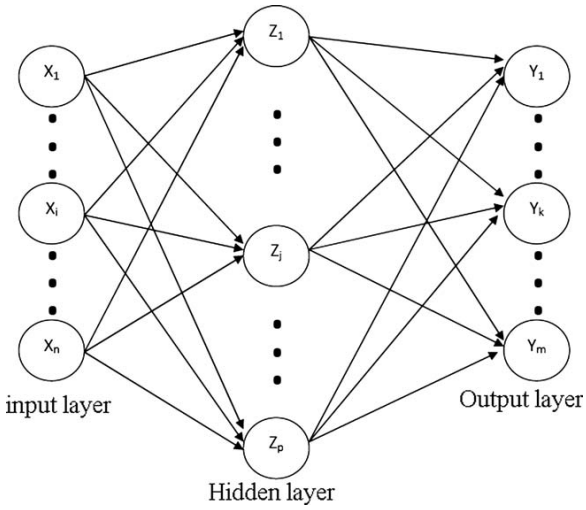

FIGURE 1. Topology of ANN with one hidden layer.

The output signal of each neuron is calculated based on the sum of the weights of all the connected signals from the previous layer plus a bias; it then generates an output according to Eq. (1) and Eq. (2).

$$Z_{in-j} = \sum_{i=1}^{n} w_{ij} x_i + v_{oj} \quad (1)$$

$$z_j = f(Z_{in-j}) \quad (2)$$

where w_{ij} is the associated weight between the i^{ih} and j^{ih} neurons, x_i is the output signal from the previous layer neuron, v_{oj} is the bias weight on the j^{ih} neuron and $f(Z_{in-j})$ is the activation function on the layer. Three customary types of activation function are tangent hyperbolic (tansig), Logarithm sigmoid (logsig) and pure line (purelin) which are shown in Eq. (3), Eq. (4) and Eq. (5) respectively.

$$f(z) = \frac{e^z - e^{-z}}{e^z + e^{-z}} \quad (3)$$

$$f(z) = \frac{1}{1 + e^{-z}} \quad (4)$$

$$f(z) = z \quad (5)$$

The available data is divided into three groups: training, validation, and testing sets. The first group is the training set, which is used for computing and updating the network weights and biases. The second group is useful when the network begins to over fit, so the error on the validation set typically raises. At this time, the training is stopped for the number of epochs for max fails and the weights and biases at the minimum of the validation error are returned. The error on the validation set is monitored during the training process. When the error on the validation set is increased, training is stopped. The last group is used to evaluate the obtained ANN during the testing stage. The test set error is not used during the training and it is also useful to plot the test set error during the training process, but when the error on validation data is raised during antiseptic epoch, the training will be stopped.

Another ANN parameter is the learning rate. The learning rate tunes the convergence of ANN during the training process, where it multiplies to back propagation errors before starting to update the weights. Small learning rates insure the better convergence of ANN, but in this case, the training process is time consuming. Larger learning rate leads to increasing convergence speed, but it may result in the uncertain ability of ANN. The momentum rate is multiplies to deviations of weights during the training process. Momentum helps convergence of ANN and decreases errors among its layers [21].

MATERIAL AND METHODS

Material

In this work, an industrial woven fabric consisting of nylon 66 as weft yarns and polyester as warp yarns was selected. The selected woven fabric was used for the production of industrial vehicle safety belts as well as industrial conveyor belts. These kinds of textiles are usually exposed to UV radiation existing in the environment. UV degradation can affect the long time performance of the materials. Technical specifications of woven fabric are shown in *Table I.*

TABLE I. Technical Specifications of woven fabrics.

Yarn Groups	Yarn Type	Thread density ($^{Ends}/_{cm}$)	Yarn crimp (%)	Yarn linear density (Den)
Warp	Polyester	16	5	900
Weft	Nylon 66	7	1	1100

Experimental Design

We used the complete block design to divide the fresh fabric to five categories [22]. A UV chamber consisting of eight ultra violet lamps from Philips TUV T8 30W/G30 were used for degradation of the fabrics. These lamps produce the ultra violet rays with the maximum wavelength of 253.7 nm. Samples were produced by cutting 50×300 mm size samples in the woven fabric in the weft, warp, and bias directions. Yarn orientation of the samples in the bias direction was 45 degrees based on elongation direction. The samples were laid inside the UV chamber under the UV lamps at the vertical distance of 15 cm. The experiments were carried out at five different exposure time levels 0, 7, 14, 21 and 28 hours (zero was the unexposed sample). At each level of exposure time, 10 samples were tested.

All samples were then dyed with C.I. Disperse blue 56 color under the same conditions [6]. To perform the dyeing process, dyeing machine AHIBA AG P_M 100 Dietikon/Zurich was used. Color analysis results with spectrophotometer TEX FLASH DATA COLOR showed the differences in color values, CIEL*C*h, at different exposure times. CIEL*C*h is one of the most common color systems in textile materials. The CIEL*C*h color space refers to the cylindrical coordinates of the CIEL*a*b* space. In CIEL*a*b* color space, in which the values L*, a* and b* are plotted using a Cartesian coordinate system. Equal distances in the space approximately represent equal color differences. L* represents lightness. This is scaled from 0, which has no lightness (absolute black), at the bottom, through 50 in the middle; to 100 which is the maximum lightness (absolute white) at the top. a* represents the red/green axis; and b* shows the yellow/blue axis.

The C* axis represents Chroma or 'saturation'. This ranges from zero at the center of the circle, which is completely unsaturated (i.e. a neutral grey, black or white) to 100 or more at the edge of the circle for very high Chroma (saturation) or 'color purity'. C* and h are calculated by a* and b* values (Eq. (6) and Eq. (7)).

$$C^* = \sqrt{(a^*)^2 + (b^*)^2} \quad (6)$$

The h represents hue angle. If we take a horizontal slice through the center, by cutting the sphere (apple) in half, we see a colored circle. Around the edge of

the circle, we see every possible saturated color (Hue). This circular axis is known as h for Hue. The units are in the form of degrees (or angles), ranging from 0 (red) to 90 (yellow), 180 (green), 270 (blue) and back to 0 (360).

$$h = \arctan\left(\frac{b^*}{a^*}\right) \quad (7)$$

Tensile responses of exposed samples were tested with using uniaxial tensile testing machine (Zwick universal testing machine-144660) under standard conditions. The tensile tests were performed in three different directions: warp, weft, and bias. The width of the samples was 50 mm and the gauge length was set to be 100 mm [23]. The sample was fixed firmly in the clamps and the stress strain curve was obtained. The test speed was 10mm/min.

Curve Fitting in Stress-Strain Curves

The data from stress-strain curves were used to find the best curve fit equation in three directions.

- **Weft direction**

A typical stress-strain curve in the weft direction is shown in *Figure 2*. In this direction, stress-strain curves at different exposure time are very close to each other. It seems that all curves follow a nearly identical path until they reach the breaking point. However, ε_{2bp} , strain in breaking points (%) is different. The color values and strain in breaking points of samples at various exposure times are shown in *Table II*.

TABLE II. Variable parameters of samples in the weft direction at various exposure times.

Exposure time(H)	ε_{2bp} (%)	Average (L*)	Average (C*)
Unexposed	30.59	37.09	40.66
7	17.95	35.28	38.15
14	10.83	34.41	35.53
21	8.75	33.62	34.26
28	4.62	32.83	33.16

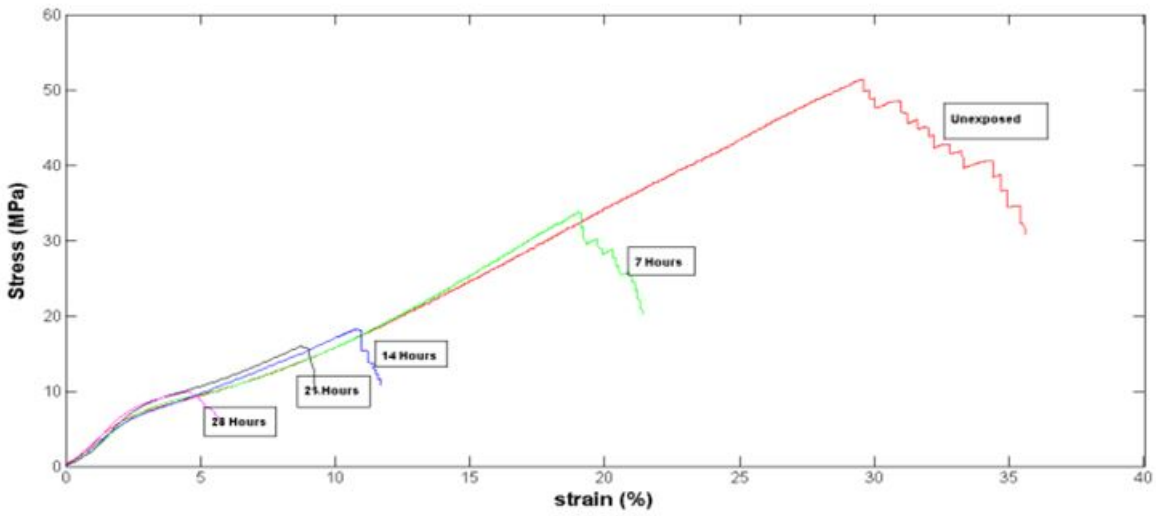

FIGURE 2. Stress-strain curves in the weft direction at various exposure times.

- **Warp direction**

Figure 3 shows stress-strain curves in warp direction. Stress-strain curves of fabrics in the warp direction show a similar trend as the weft direction. The breaking stress and breaking strain are nearly the same for all exposure times. It shows that UV radiation has no significant effect on tensile property in the warp direction. The reason for this is that the UV radiation does not affect the tensile property of polyester yarn in warp direction significantly.

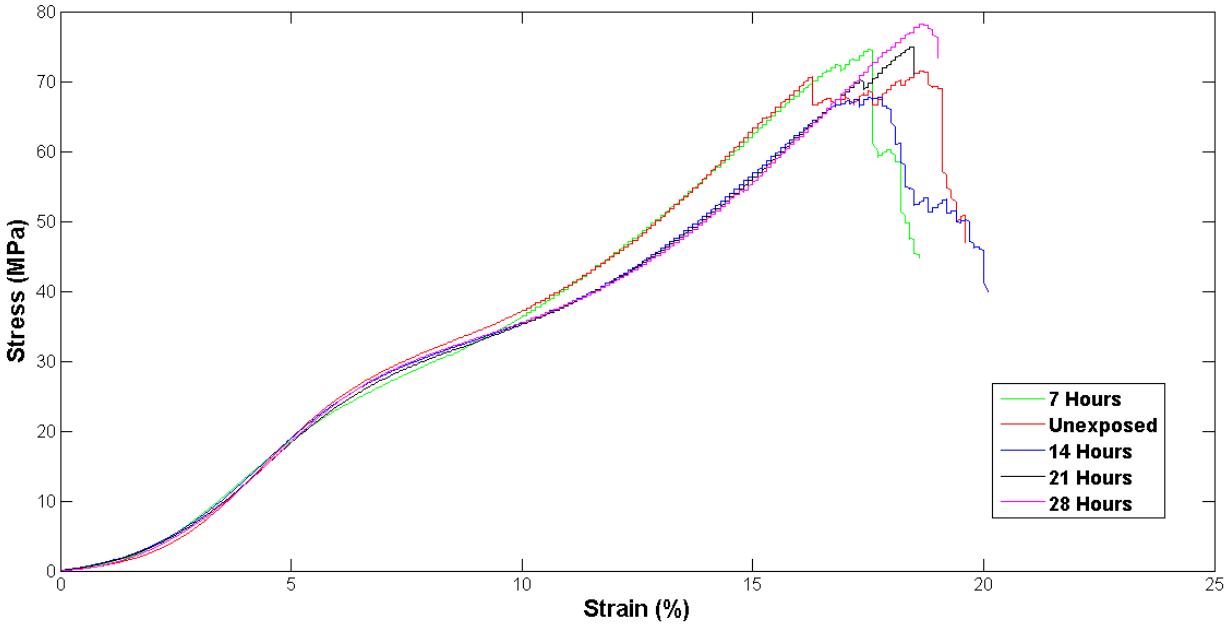

FIGURE 3. Stress-strain curves in the warp direction at various exposure times.

- **Bias direction**

Stress-strain curves in the bias extension are shown in *Figure 4*. As can be seen the curves are significantly different from each other. The results of the curve fitting process show that the curve can be divided in two different parts as shown in Eq. (8). In the first part, up to the locking point, the stress-strain curve is fitted with an exponential function. In the second part, from the locking point up to the breaking point, the stress-strain curve has a linear behavior.

$$\sigma_s = \begin{cases} A\times(\exp(B\times\varepsilon_s)-1) & 0 \le \varepsilon_s \le \varepsilon_{sl} \\ C\times(\varepsilon_s-\varepsilon_{sl})+\sigma_{sl} & \varepsilon_{sl} < \varepsilon_s \le \varepsilon_{sbp} \end{cases} \quad (8)$$

where, ε_s is shear strain (%), σ_s is shear stress (MPa), ε_{sl} is shear strain in the locking point, σ_{sl} is stress at ε_{sl} , ε_{sbp} is shear strain in the breaking point. Thus, the strain-stress curve can be defined by five responses or parameters. These include shear strain at breaking point (ε_{sbp}), shear strain at locking point (ε_{sl}) and three constants A, B and C. These parameters are determined for each individual exposure time. Color values and variable parameters of samples in bias direction at various exposure times are shown in *Table III*.

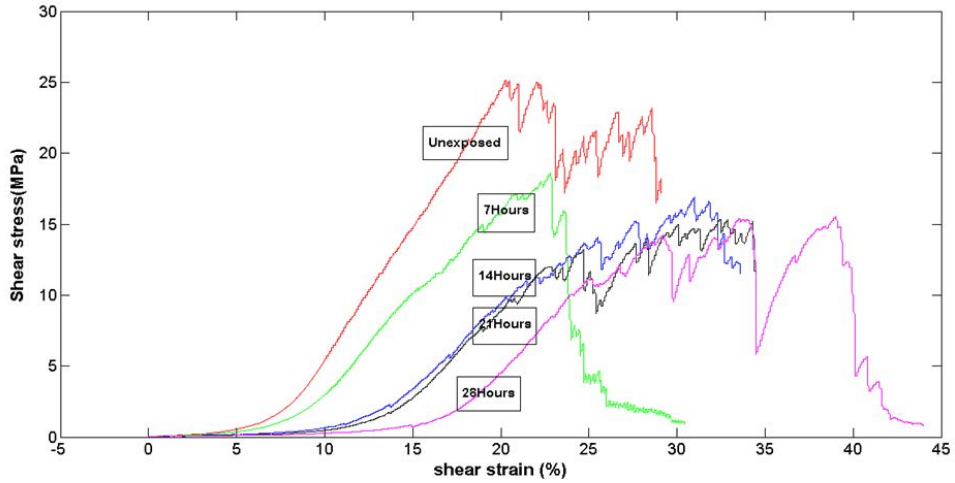

FIGURE 4. Stress-strain curves in the bias direction 45 at various exposure times.

TABLE III. Variable parameters of samples in the bias direction 45 at various exposure times.

Exposure time(H)	Parameter (A)	Parameter (B)	Parameter (C)	ε_{sl} (%)	ε_{sbp} (%)	Average (L*)	Average (C*)
Unexposed	0.072	0.441	1.86	9.10	20.27	37.09	40.66
7	0.070	0.374	1.27	10.55	22.83	35.28	38.15
14	0.032	0.349	1.22	14.05	24.56	34.41	35.53
21	0.016	0.342	1.20	14.59	24.75	33.62	34.26
28	0.006	0.332	1.19	17.97	25.81	32.83	33.16

RESULTS AND DISCUSSION

In each exposure time, average color values were determined by the spectrophotometer. We considered the two most significant factors, L* and C*, as dependent variables. A diagram of spectrophotometer results is shown in *Figure 5*.

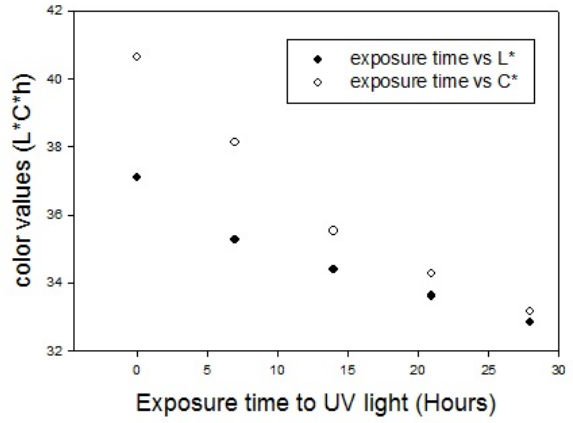

FIGURE 5. Color values at different exposure times.

Determination of Stress -Strain Parameters from Regression Method

- **Weft direction**

In each case of exposure time, the correlation between the strains at the breaking point with color values was determined. L* and C* were defined as dependent variables. Strain in the weft direction (ε_{2bp}) was defined as response or the independent variable. The multiple regression model used is based on the least squares method. Eq. (9) shows the quadratic regression equation for ε_{2bp}. The correlation coefficient R- Squares was 0.98. The three dimensional regression curves are shown in *Figure 6*.

$$\varepsilon_{2bp}\,(\%) = -358.692 + 54.6514 \times (L^*) - 34.7172 \times (C^*) - 0.7849 \times (L^*)^2 + 0.516 \times (C^*)^2 \quad (9)$$

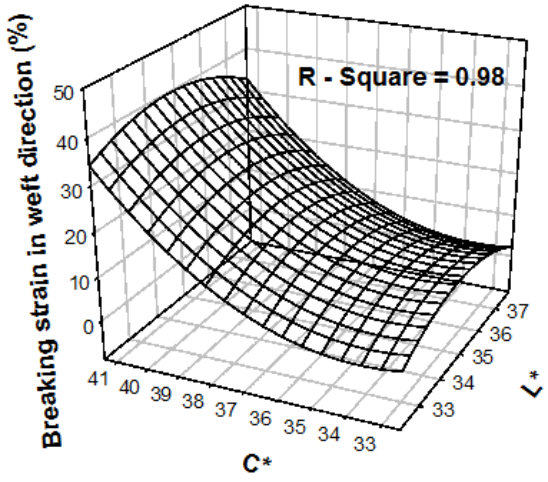

FIGURE 6. 3D regression curve for the breaking strain.

Bias direction

In each case of exposure time, the correlations between each parameter with color values were determined. L* and C* were defined as dependent variables. ε_{sbp} , ε_{sl}, parameter (A) , parameter (B) and parameter (C) were defined as independent (response) variables. The multiple regression model used which is based on the least squares method. Eq. (10) shows the plane regression equation for parameter (A) and Eq. (11) through Eq. (14) show quadratic regression equations for parameter (B), Parameter (C), ε_{sl} and ε_{sbp} respectively. The three dimensional regression curves as well as regression coefficients R-squares are shown in *Figure 7*.

$$Parameter\ (A) = 0.0545 - 0.0242 \times (L^*) + 0.0226 \times (C^*) \quad (10)$$

$$Parameter\ (B) = -2.4746 + 0.4509 \times (L^*) - 0.2923 \times (C^*) - 0.0063 \times (L^*)^2 + 0.0041 \times (C^*)^2 \quad (11)$$

$$Parameter\ (C) = -18.9127 + 4.2637 \times (L^*) - 3.077 \times (C^*) - 0.059 \times (L^*)^2 + 0.0418 \times (C^*)^2 \quad (12)$$

$$\varepsilon_{sl}(\%) = 52.2837 + 10.5463 \times (L^*) - 11.9116 \times (C^*) - 0.122 \times (L^*)^2 + 0.1319 \times (C^*)^2 \quad (13)$$

$$\varepsilon_{sbp}\ (\%) = 102.0079 - 13.4114 \times (L^*) + 8.398 \times (C^*) + 0.2177 \times (L^*)^2 - 0.136 \times (C^*)^2 \quad (14)$$

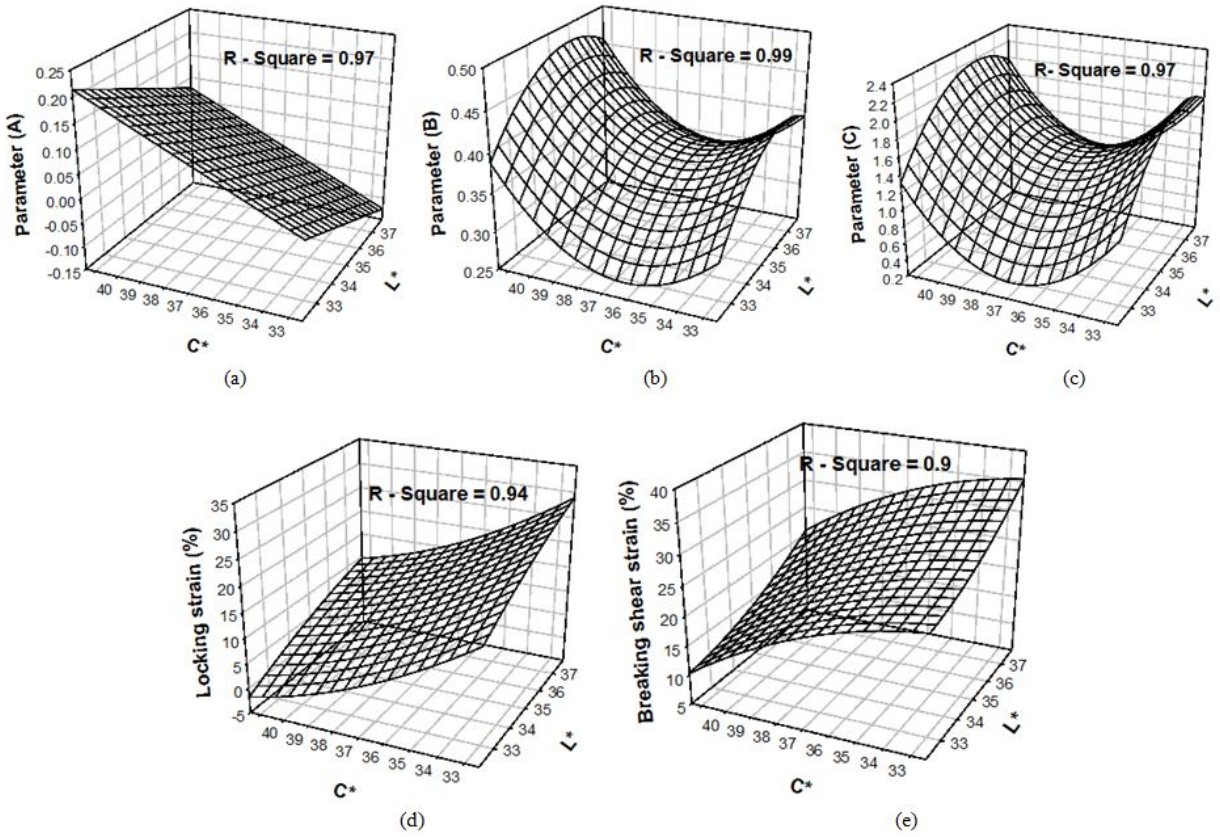

FIGURE 7. 3D curves and regression coefficients R-squares in the bias extension test.

Determination of Stress-Strain Parameters from ANN Method

These data were fed to three different neural network programs along with the color value for training; one for the prediction of parameter A and B; another for the predicting the parameter C and locking strain.

The last network was used for prediction of the breaking strain in the weft and bias direction. The neural network was a multilayered network. The training algorithms were back propagation (Levenberg-Marquardt). The topologies of the networks are shown in *Figure 8*.

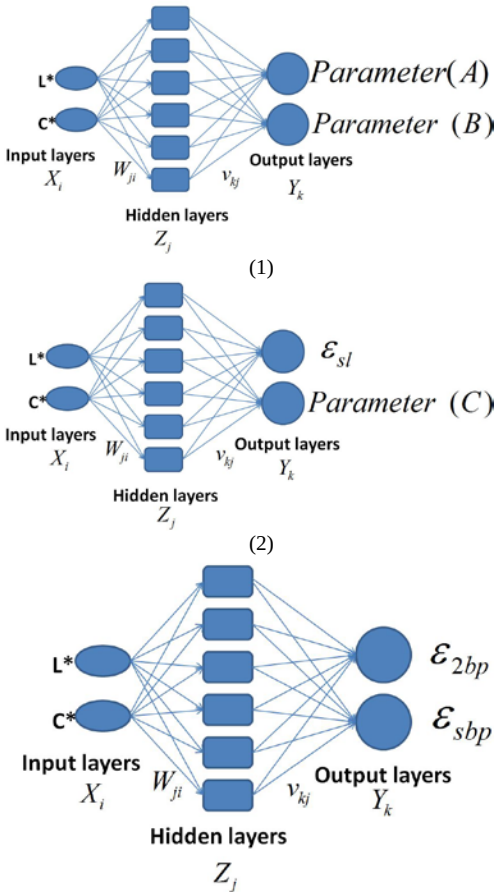

FIGURE 8. The topology of used neural network used.

The programs were written in Matlab 7.0. Input and output data are shown in *Table II and III*. All the sample indexes were scaled to be in the set of [-1, 1] before training. All connection weights and biases were initialized randomly between -1 to 1. The networks specifications are shown in *Table IV*. Various neural networks with different network parameters such as topology, learning rate, momentum, training rule, and activation function were experienced by the trial- error method. Among all trained networks, only Levenberg- Marquardt (trainlm) with the topology of single hidden layer (2-6-2) had acceptable performance, whereas training data were scaled between -1 to 1. Therefore, suitable activation function was tangent hyperbolic (tansig).

Changes in weights on network nodes for each input and output layer are effective factors in the sensitivity analysis of that input and output. Eq. (15) and Eq. (16) calculate the sensitivity of each input and output variable that constitutes the effect of connection weights of each input and output. Results of sensitivity analysis are presented in *Table V*.

$$Effective\ percent\ of\ each\ input\ variable = \frac{sum\ of\ the\ weight\ of\ each\ input\ node}{sum\ of\ the\ weight\ of\ total\ input\ nodes} \quad (15)$$

$$Affected\ percent\ of\ each\ output\ variable = \frac{sum\ of\ the\ weight\ of\ each\ output\ node}{sum\ of\ the\ weight\ of\ total\ output\ nodes} \quad (16)$$

TABLE IV. Networks specifications.

Networks	momentum	Learning rate	Topology	Activation function			Training rule	Training epocks
				Input layer	Hidden layer	Output layer		
1	0.9	0.01	2-6-2	tansig	tansig	purelin	Trainlm	2584
2	0.9	0.01	2-6-2	tansig	tansig	purelin	Trainlm	646
3	0.9	0.01	2-6-2	tansig	tansig	purelin	Trainlm	498

TABLE V. Sensitivity test data (in percent) of networks for input and output data.

Sensitivity	Network 1	Network 2	Network 3
Effect of L* (%)	37.40	38.75	38.04
Effect of C* (%)	62.60	61.25	61.96
Affected Parameter (A) %	54.42	-	-
Affected Parameter (B)%	45.58	-	-
Affected Parameter (C)%	-	52.46	-
Affected ε_{sl} (%)	-	47.54	-
Affected ε_{2bp} (%)	-	-	55.64
Affected ε_{sbp} (%)	-	-	44.36

In the training stage of the ANN model, three groups of data were introduced to the ANN as 80% training, 10% validation, and 10% testing data. Statistical parameters such as the correlation coefficient between the actual and predicted test results of the woven fabric, mean square error for training, validation, and testing data and mean absolute error for test data were calculated to assess the performance of ANN models. The results are shown in *Table VI*.

TABLE VI. Statistical results showing of prediction performance of models.

Statistical parameters	Network1	Network2	Network3
Correlation coefficient R	0.985	0.992	0.996
Mean squared error (MSE) train	1.76×10^{-3}	0.64×10^{-3}	0.45×10^{-3}
Mean squared error (MSE) validation	0.79	0.43	0.12
Mean squared error (MSE) test	1.23	0.56	0.52
Mean absolute percent error (MAPE)	4.0	2.7	2.3
Cases with more than 10% error	0	0	0

Model Validation

To validate the method in the bias direction, a new category of fabric was produced with the specific time of UV radiation at the same condition, 24 hours. In this category, 10 samples were produced and tested. After the dyeing process, CIE L*C*h color values were determined (L*=33.2297 and C*=33.7115). The unknown parameters were estimated by regression equations (Eq. (9) to Eq. (14)) and ANN models. These estimated values were considered in Eq. (8) and the predicted curves were obtained. The average values of the estimated parameters for validating the samples are shown in *Table VII*. The validating samples were then tested with the tensile testing machine. The test results were compared with regression and ANN predicted curves as shown in *Figure 9*. As can be seen the predicted curves are close to the experimental curve with significant accuracy. More deviation of the experimental curve from the predicted curves is observed after the locking point. In this region, some slippage occurs between warps and wefts. This slippage phenomenon may be a source of error leading to deviation of the experimental curve form the theoretical curves. However, the experimental curves are very close to the predicted curves. It can be concluded that the proposed methods can predict the mechanical properties of UV degraded fabric with acceptable accuracy.

TABLE VII. The regression and ANN estimated parameters.

model	Parameter (A)	Parameter (B)	Parameter (C)	ε_{sl} (%)	ε_{sbp} (%)	ε_{2bp} (%)
ANN	0.0108	0.3384	1.1912	15.7724	25.1737	7.1196
Regression	0.0122	0.3379	1.2001	16.3618	25.2881	6.7081

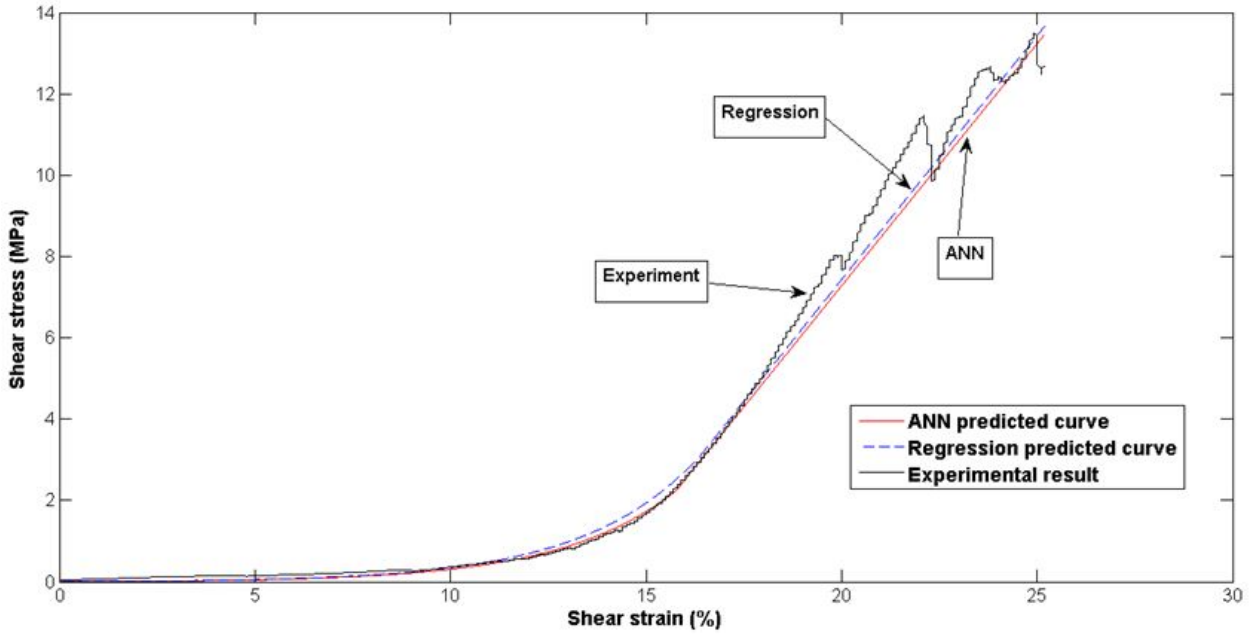

FIGURE 9.Stress-strain curves of the 24 hours exposure time in the bias direction.

CONCLUSION

In this work, the mechanical properties of a woven fabric exposed to UV radiation were investigated. Five different exposure times were used. The degraded samples were then dyed in identical dyeing conditions. In each case of exposure time, the color values and tensile parameters in the weft and bias directions were obtained. The ANN and regression methods were used to correlate the color values with the tensile parameters. The multiple regression equation shows high regression coefficient R-Squares (0.9 to 0.99), for each tensile property. Three ANN programs with back propagation algorithm were trained, showing minimum error for all of them, and tested. To validate the model in the bias direction, one new fabric was exposed to specific exposure time. Ten samples from this validation category were tested. The theoretical equations of stress-strain were calculated by two methods and the predicted stress-strain curves were obtained. The predicted curves were then compared with the experimental stress-strain curve. The results show that the experimental curve is very close to the predicted curves. The results also revealed that ANN predicted curve is closer than the regression predicted curve to the experimental curve. This shows that the proposed methods can predict the tensile properties of UV degraded fabrics with acceptable accuracy.

REFERENCES

[1] Ghane, M.; Hosseini Ravandi, S.A.; Moezzi, M.;Evaluation of diamond bar patterns on fabric surface using an image analysis technique; *Journal of the Textile Institute* 2010, 101,2-7.

[2] Shamey, R.; Sinha, K.; A review of degradation of nylon 6. 6 as a result of exposure to environmental conditions; *Review of Progress in Coloration and Related Topics*2003,33,93-107.

[3] Zhang, H.; Zhang, J.; Chen, J.; Hao, X.; Wang, S.; Feng, X.; Guo,Y.;Effects of solar UV irradiation on the tensile properties and structure of PPTA fiber; *Polymer Degradation and Stability*2006, 91, 2761-2767.

[4] Liu, Y.; Hu, H.;A review on auxetic structures and polymeric materials; *Scientific Research and Essays* 2010,5 ,1052-1063.

[5] Sargunamani D.; Selvakumar N.; Effect of Ozone Treatment on the Dyeing Properties of Mulberry and Tassar Silk Fabrics; *Journal of Engineered Fibers and Fabrics*2012;7,21-27.

[6] Nunn, D. M.;*The Dyeing of synthetic-polymer and acetate fibres*; Dyers Co. Publications Trust : distributed by the Society of Dyers and Colourists; Bradford, West Yorkshire, 1979.

[7] Vangheluwe, L.;Relaxation and inverse relaxation of yarns after dynamic loading;*Textile Research Journal*1993;63, 552-556.
[8] Żurek, W.; Aksan, S.; A rheological model of viscose rayon; *Journal of Applied Polymer Science*1975;19, 3129-3137.
[9] Manich, A. M.;Visco-elastic behaviour of polypropylene fibres; *Textile Research Journal* 1999;69,325-330.
[10] Serwatka, A.; Bruniaux, P.; Frydrych, I.;New Approach to Modeling the Stress-Strain Curve of Linear Textile Products. Part 1 – Theoretical Considerations; *Fibers & Textiles in Eastern Europe*2006;14, 30 – 35.
[11] Montogomery, D. C.; Peck, E. A.; Vining, G. G.; *Introduction of Linear Regression Analysis*, 5th ed.; Wiley Series in Probability and Statistics; Hoboken, New Jersey, 2012.
[12] Abghari, R.; Shaikhzadeh Najar, S.; Haghpanahi, M.; Latifi, M.; Contributions of in-plane fabric tensile properties in woven fabric bagging behavior using a new developed test method; *International Journal of Clothing Science and Technology*2004;16,418-433.
[13] Almetwally, A. A.; Salem, M. M.; Comparison between Mechanical Properties of Fabrics Woven from Compact and Ring Spun Yarns; *AUTEX Research Journal*2010, 10, 35-40.
[14] Malik, Z. A.; Malik, M. H.; Hussain, T.; Arain, F. A.; Development of Models to Predict Tensile Strength of Cotton Woven Fabrics; *Journal of Engineered Fibers and Fabrics*2011; 6, 46-53.
[15] Kotb, N. A.; The Perception of Plain Woven Fabrics' Performance Using Regression Analysis; *Journal of Basic Applied Scientific Research*2012*;* 2, 20-26.
[16] Kannappan, S.; Dhurai, B.; Investigating and Optimizing the Process Variables Related to the Tensile Properties of Short Jute Fiber Reinforced with Polypropylene Composite Board; *Journal of Engineered Fibers and Fabrics*2012;7,28-34.
[17] Zeydan, M.; Modeling the woven fabric strength using artificial neural network and Taguchi methodologies; *International Journal of Clothing Science and Technology*2008*;* 20,104-118.
[18] Ertugrul, S.; Ucar, N.; Predicting Bursting Strength of Cotton Plain Knitted Fabrics Using Intelligent Techniques; *Textile Research Journal*2000*;*70, 845-851.
[19] Hadizadeh, M.; Jeddi, A.A.A.; Tehran, M.A.; The Prediction of Initial Load-extension Behavior of Woven Fabrics Using Artificial Neural Network; *Textile Research Journal*2009*;* 79, 1599-1609.
[20] Hadizadeh, M.; Tehran, M. A.; Jeddi, A. A. A.; Application of an Adaptive Neuro-fuzzy System for Prediction of Initial Load—Extension Behavior of Plain-woven Fabrics; *Textile Research Journal*2010, 80, 981-990.
[21] Krose B and Smagt P; *An Introduction to Neural Networks*. 8th ed; The University of Amsterdam: Amesterdam. Netherland; 1996.
[22] Montogomery. D.C.; *Design and Analysis of Experiments*, 7th ed.; John Wiley & Sons; Hoboken, New Jersey, 2008.
[23] Cao, J.; Akkerman, R.; Boisse, P.; Chen, J.; Cheng, H.S.; de Graaf, E.F.; Gorczyca, J.L. ; Harrison, P.; Hivet, G.; Launay, J.; Lee, W.; Liud, L.; Lomov, S.V.; Long, A.; de Luycker, E.; Morestin, F.; Padvoiskis, J.; Peng, X.Q.; Sherwood, J.; Stoilova, T.Z.; Tao, X.M.; Verpoest, I.; Willems, A.; Wiggers, J.; Yu, T.X.; Zhu, B.; Characterization of mechanical behavior of woven fabrics: Experimental methods and benchmark results; *Composites*: *Part A: Applied Science and Manufacturing*2008*;*39,1037–1053.

AUTHORS' ADDRESSES

Meysam Moezzi
Mohammad Ghane
Dariush Semnani
Isfahan University of Technology
Department of Textile Engineering
Isfahan, Isfahan 83111
IRAN